

Simulation of the structure and stability of sphalerite (ZnS) surfaces

K. WRIGHT,¹ G.W. WATSON,² S.C. PARKER,² AND D.J. VAUGHAN¹

¹Department of Earth Sciences, University of Manchester, Oxford Road, Manchester M13 9PL, U.K.

²Department of Chemistry, University of Bath, Claverton Down, Bath BA2 7AY, U.K.

ABSTRACT

Atomistic simulation techniques were used to investigate the surface energies and stabilities of the sphalerite form of ZnS. The results show that for pure ZnS the lowest energy surfaces are type I and all of the form {110} with a calculated surface energy of 0.65 J/m². In addition, we illustrate how type III surfaces, such as {111}, can be stabilized with respect to {110} by the introduction of point defects to the surface layer. Such defects lead to changes in stoichiometry and to the valence state of surface species. In general, the results suggest that for Zn-poor surface stoichiometries, the (111) surface becomes the most stable, whereas for Zn-rich compositions the (111) is stabilized to the greatest extent.

INTRODUCTION

Sphalerite or zincblende, the cubic form of ZnS, has been widely studied because of numerous technological applications and economic importance. Sphalerite is found in nature in hydrothermal and sedimentary exhalative ore deposits where it normally contains significant amounts of other metals substituting for Zn, including Cd, Co, Ni, In, Ga, Ge, and most commonly Fe. It is of economic importance because it is the major source of Zn, Cd, In, Ga, and Ge. Industrially, sphalerite and its hexagonal polytype wurtzite, are used in water purification systems, luminescent displays, and solar cells. Nickel (1965) gives a useful review of the physical properties of ZnS.

Use of sphalerite and its structural analogues as semiconductors prompted several studies on the surface structure of these materials. In particular, the {110} perfect cleavage surface attracted considerable attention. Studies using X-ray photoelectron spectroscopy (XPS), low energy electron diffraction (LEED), and theoretical methods have shown that the ZnS {110} surface undergoes considerable relaxation and reconstruction from the bulk termination (see Duke 1988 for a review), with movement of the Zn atoms down into the surface structure. Furthermore, this phenomenon is observed in other semiconductor compounds with the sphalerite structure (e.g., GaAs, ZnSe, CdTe). The above observations led to the concept of a universal {110} surface structure for sphalerite structure semiconductors (Duke 1988). Duke and Wang (1988), by using tight-binding models, were able to extend this work to wurtzite structure (1010) and (1120) cleavage surfaces that show a similar reconstruction.

The {110} surfaces, however, are not always observed in the external crystal morphology. It is more common to see external surfaces based on tetrahedra [i.e., {111} type] or combinations of tetrahedra and dodecahedra. Growth of synthetic sphalerite by chemical transport

(e.g., Matsumoto and Shimaoka 1986) leads to the formation of {111} as the dominant surface. The surface energy is likely to be an important factor in controlling morphology during growth, especially in the early stages when crystal size is small and the surface-to-bulk ratio is large. Yoshiyama et al. (1988) used a phenomenological approach to determine the effects of surface energy on the thin-film orientation of ZnS, CaS, and SrS. Their calculations indicate that for ZnS thin films, the (111) plane has the lowest surface energy. First principles calculations have been used to study (100) surface reconstructions in ZnSe as a function of Zn activity (Garcia and Northrup 1994), and suggest that surface energies, hence their relative stability, depend on the chemical potential of Zn.

This paper uses atomistic simulation techniques to model surfaces of the sphalerite phase of ZnS. These techniques, based on the Born model of solids, have been previously employed to study the surface structures and reactivity of a range of oxide materials (e.g., Colbourne 1992; Davies et al. 1994) and carbonates (Parker et al. 1993). In this study, we first calculate the geometry and surface energy of the {001}, {110}, and {111} surfaces in sphalerite, taking all the different surface terminations into account, and then consider the effects of non-stoichiometry on surface stability.

METHODOLOGY

The computer code METADISE (Watson et al. 1996) was used to perform simulations on the surfaces of ZnS. The approach treats the crystal as planes of atoms that are periodic in two dimensions. Surfaces are modeled by considering a single block, whereas two blocks together simulates the bulk or more complex interfaces as shown in Figure 1. The simulation is facilitated by dividing the cell into two regions, a near-surface region, Region 1, composed of those atoms adjacent to the surface or interface, and an outer region, Region 2 (see Fig. 1). The

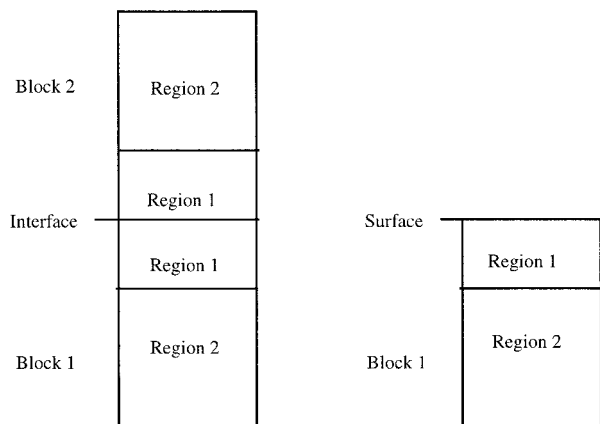


FIGURE 1. Schematic representation of the two region approach used to model an interface between two blocks and a single surface block.

ions in Region 1 are allowed to relax to their minimum energy configuration, whereas the ions of Region 2 are fixed at their bulk equilibrium positions. In all cases, the calculations were carried out on fully converged region sizes. The forces on the ions are calculated within the Born model of solids in which effective interatomic potentials are used. This model includes long-range contributions from the Coulombic interactions, summed using the two-dimensional Parry method (Parry 1975, 1976) and short range interactions because of the overlap of electron clouds. These short range interactions can be modeled well by the Buckingham potential:

$$U_{ij} = \sum_{ij} A_{ij} \exp\left[\frac{r_{ij}}{\rho_{ij}}\right] - C_{ij} r_{ij}^{-6} \quad (1)$$

where i and j are two ions with separation r . A and ρ are constants describing repulsion, and C is a term that takes dispersion effects into account. In addition, the shell model of Dick and Overhauser (1957) has been used to model the polarizability of the S ion, and a three-body term is included to describe the directionality of the S-Zn-S bonds. All of the parameters used in this study were derived by empirical fitting to crystal properties (Wright and Jackson 1995) and are presented in Table 1. These parameters have been used successfully to model the defect behavior of both the sphalerite and wurtzite polymorphs of ZnS (Wright and Jackson 1995).

The specific surface energy is defined as the energy per unit area required to form the crystal surface relative to the bulk. The surface energy (γ) is therefore given by:

$$\gamma = \frac{U_s - U_b}{A} \quad (2)$$

where U_s refers to the energies of Region 1 for the surface, U_b refers to the energy of an equivalent number of bulk atoms, and A is the surface area.

A requirement for this calculation is that the unit cell does not have a dipole perpendicular to the surface be-

TABLE 1. Potential parameters

Parameter	S-S	Zn-S
A (eV)	1200.000	528.889
r (Å)	0.149	0.411
C (eV Å ⁶)	120.000	0.000
Shell model		
K_s (eV Å ⁻²)	16.860	2.181
Three-body terms		
S-Zn-S three-body force constant (eV rad ⁻²)		0.713
S-Zn-S three-body angle (degrees)		109.470

Notes: The short range potential cutoff was set to 12 Å.

cause such a dipole, when repeated into the crystal, results in divergence of the surface energy. Tasker (1979) defined three types of surface (I, II, and III) that are illustrated in Figure 2. Type I surfaces (Fig. 2a) are composed of stoichiometric layers and thus have no dipole perpendicular to the surface. Type II surfaces (Fig. 2b) are composed of multi-layer repeat units that have no overall dipole. In contrast, type III surfaces (Fig. 2c) cannot be cleaved between layers to give a non-dipolar surface. Type III surfaces should therefore be unstable; however, recent work on NiO (Oliver et al. 1995) and MgO (Watson et al. 1996) have shown that oxidation or reconstruction to remove the dipole can stabilize these surfaces. The most common reconstruction is to cleave the surface through a layer, transferring half of the ions from the top of the repeat unit to the bottom: This mechanism removes the dipole on the {111} surface of rock salt structure materials (Tasker 1979).

Crystal morphology can be predicted from the surface energies using Wulff's theorem (Wulff 1901) in which the equilibrium form of a crystal for a given volume possesses minimal surface energy. Hence, the morphological importance of a crystal face is proportional to its specific surface energy.

RESULTS

The simulated crystal structure of sphalerite was "cut" to produce {110}, {001}, and {111} type surfaces. Not all surfaces of a given form are equivalent, and in many cases it is possible to have more than one repeat unit for a particular (hkl) surface. In particular, the tetrahedral symmetry of sphalerite is such that opposite senses of the [111] direction are not equivalent. In sphalerite, only the {110} surfaces can be classified as type I, all of the other surfaces studied are type III. To remove the dipole, a fraction of the top plane of atoms has to be removed to the base of the repeat unit. The structure of each surface studied is shown schematically in Figure 3 and the associated relaxed and unrelaxed surface energies are given in Table 2. In the case of {110}, all surfaces of this form have the same repeat unit, and all have the same surface energy. The {001} and {111} type surfaces can be cut in two different ways to remove the dipole. The labels (hkl) S and (hkl) Zn correspond to S and Zn terminated surface cuts, respectively. It should be noted that the (001) S and

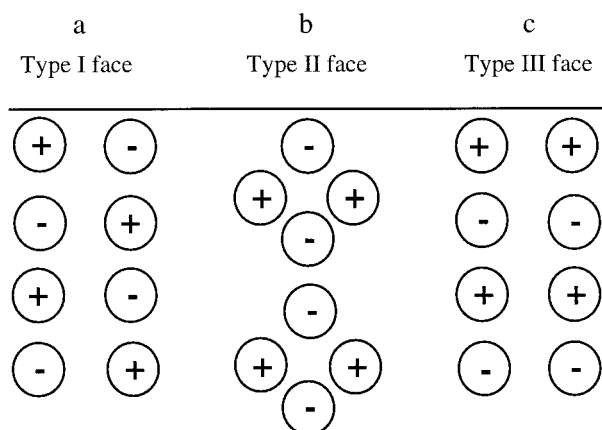


FIGURE 2. The three different types of surface, after Tasker (1979). (a) Type I surfaces consisting of neutral planes of ions. (b) Charged planes with no residual dipole in the repeat unit. (c) Charged planes that possessing a net dipole that must be removed by reconstruction.

Zn terminated planes are identical to the (010) and (100) S and Zn terminated planes. However, for simplicity, we include results only for (001).

The most striking feature of Table 2 is the difference in the unrelaxed and relaxed surface energies. In particular, the (111)S and $(\bar{1}\bar{1}\bar{1})$ Zn surfaces show a reduction in energy of more than 60%. There is also a marked difference in the relaxed surface energies of the other {111} terminations, with the $(\bar{1}\bar{1}\bar{1})$ Zn being the most energetically favorable. The {110} surfaces, however, have the lowest energy (0.65 Jm^{-2}) and are thus predicted to be the most stable. The calculated relaxed and unrelaxed surface structures in Figure 4 illustrate the amount of movement that takes place on relaxation. Duke et al. (1984) used five independent structural parameters to describe the {110} surface geometry, on the basis of displacements parallel to and normal to the uppermost layers. These are based upon relative spacings between anions and cations and changes in the spacings between layers. Our calculations predict an upward movement of 0.047 \AA for S with a corresponding downward movement of 0.24 \AA for Zn as shown in the inset of Figure 4b. The values are about half of those predicted by Duke et al. (1984) who found movements of $+0.08$ and -0.51 \AA for S and Zn, respectively. The predicted values for atom movements parallel to the upper layers, however, are in close agreement with those of Duke et al. (1984).

In nature, sphalerite commonly has a tetrahedral or dodecahedral form displaying {111}, {122}, and {110} faces such that complex intergrowths of tetrahedral and dodecahedral forms often occur. Synthetical crystals commonly exhibit {111} type faces (Matsumoto and Shimaoka 1986). Although {110} is the perfect cleavage surface and has the lowest predicted surface energy, it is not the most commonly observed face in the external crystal morphology. However for surfaces such as {111} to become dominant they must be stabilized in some way rel-

	(001)S	D	(001)Zn
	--S--	0.00	-Zn--
	-Zn--Zn-	0.26	--S---S--
	--S---S--	0.50	-Zn--Zn-
	-Zn--Zn-	1.00	--S---S--
	--S--	1.26	-Zn-
	(110)		
	-Zn--S--Zn--S	0.00	
	-Zn--S--S--Zn	0.36	
	(111)Zn		$(\bar{1}\bar{1}\bar{1})$ S
	-Zn-	0.00	-S--
	-S---S---S---S--	0.44	-Zn--Zn--Zn--Zn
	-Zn--Zn--Zn--Zn	0.58	-S---S---S---S--
	-S---S---S---S--	1.01	-Zn--Zn--Zn--Zn
	-Zn--Zn--Zn	1.15	--S---S---S--
	(111)S		$(\bar{1}\bar{1}\bar{1})$ Zn
	-S---S---S--	0.00	--Zn--Zn--Zn--
	-Zn--Zn--Zn--Zn	0.14	-S---S---S---S--
	-S---S---S---S--	0.57	-Zn--Zn--Zn--Zn-
	-Zn--Zn--Zn--Zn	0.72	-S---S---S---S--
	--S--	1.15	-Zn-

FIGURE 3. Schematic illustration of the surface repeat unit of each of the surfaces studied. D (in center) is the depth below the surface of each layer of atoms in lattice units (lu) where $1 \text{ lu} = 5.41 \text{ \AA}$.

ative to {110}. Sphalerite normally exhibits small deviations from stoichiometry (Scott and Barnes 1972) and thus excess S or Zn at the surface could lead to changes in the surface energy as has been predicted by Garcia and Northrup (1994) for ZnSe. To simulate this situation, the energies of selected surfaces containing point defects were computed. First we consider reactions that could result in the growth of a defective layer.

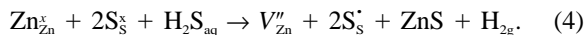
Several reactions can occur under hydrothermal conditions whereby point defects (vacancies and interstitials) are introduced into the surfaces of sphalerite. First, we consider reactions leading to a S-rich stoichiometry. In the system S-H₂O at low pH, H₂S_{aq} is a stable species and can react with ZnS in a number of ways.



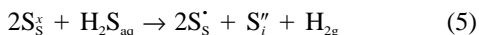
In Equation 3, H₂S dissociates and molecular H forms. A Zn ion is removed from its lattice site and combined with the S²⁻ ion to form a unit of ZnS. A Zn vacancy is formed at the surface and charge balance is maintained by oxidation of S²⁻ to S⁻. In defect notation (Duke et al. 1984) this can be written as:

TABLE 2. Unrelaxed (Eu) and relaxed (Er) surface energies (J/m^2) in pure, stoichiometric ZnS

Surface	(001) S	(001) Zn	(110)	(111) Zn	(111) S	($\bar{1}\bar{1}\bar{1}$) S	(111) Zn
Eu	2.72	2.67	1.18	2.80	2.84	2.84	2.80
Er	1.31	1.25	0.65	1.82	1.12	1.89	1.03



Here, V_A and A_i refer to a vacancy and interstitial of species A , respectively. The superscripts denote charge associated with the defect that can be neutral (x), positive (\bullet), or negative ($'$). We calculate the energy of reaction one (E_{R1}) in the appendix by summing all of the appropriate energy terms which gives a value of -40.709 eV for this reaction excluding the contribution from the specific surface. Additionally, the S^{2-} ion released from the dissociation of H_2S could simply enter the surface layer as an interstitial species where the reaction is written as:

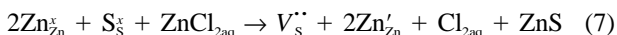


and the energy of this second reaction (E_{R2}) is -4.285 eV, again neglecting the surface specific component.

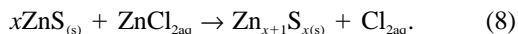
Next we consider reactions involving species such as ZnCl_2 leading to a Zn-rich stoichiometry as:



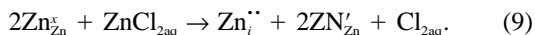
This leads to the formation of S vacancies at the surface:



and has a reaction energy (E_{R3}) of -39.559 eV. In this case, charge balance is maintained by reduction of Zn^{2+} to Zn^+ . Finally, excess Zn can be introduced into the system as interstitial Zn by reaction with ZnCl_2 .

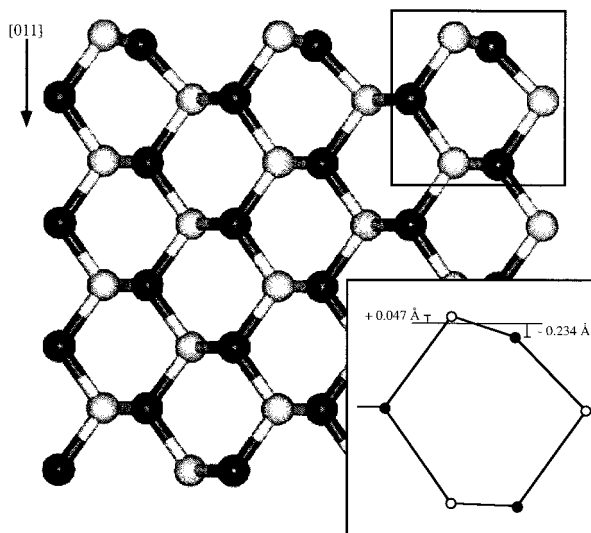


Or, in defect notation



For this fourth reaction the energy (E_{R4}) is -2.02 eV. In nature, many other reactions are possible, depending on the Eh/pH of the fluid and the dominant aqueous species. However those possibilities above are representative and cover all vacancy and interstitial possibilities.

Using these reactions, we can calculate the energy of reaction for the various defective surfaces and assess their stabilities relative to the $\{110\}$ case. The effective surface energy (E_{eff}) is defined as the difference between the pure surface structure and the surface layer containing defects plus the energy of the reaction leading to the formation of the defects. The results (Table 3) predict that for Zn poor compositions the (111) surfaces are more stable than the $\{110\}$, whereas for Zn-rich compositions the $(\bar{1}\bar{1}\bar{1})$ face is stabilized relative to $\{110\}$. Table 3 shows the energy of formation of the different defect clusters at the surface and in the bulk crystal. The difference between the two is the segregation energy, which indicates, in this case, that defects migrate to the surface because surface

**FIGURE 4.** The structure of the (011) surface after relaxation. The inset is an exaggerated sketch showing the degree of movement of light spheres (S) and dark spheres (Zn).

formation energies are lower than in the bulk. The reaction energies given in Table 3 are those specific to a particular reaction occurring at a particular surface and are found by summing the reaction energies calculated in Equations 3–5 with the defective surface energy. Thus reactions involving the formation of interstitials on any surface are unfavorable.

DISCUSSION

For small crystals, the ratio of surface to bulk is large and thus surface energies largely determine which planes develop. The most stable planes are those with the lowest surface energy. In a study aimed at the growth of thin films, Yoshiyama et al. (1988) calculated surface energies for ZnS, CaS, and SrS. Their calculations were based on nucleation theory and the assumption that surface energy is approximately proportional to the number of dangling bonds present. For sphalerite type ZnS, the above authors identified two kinds of (111) surface, one with a single dangling bond and the other with three dangling bonds that correspond to Zn and S terminated surfaces, respectively. The $(111)\text{Zn}$ plane had the lowest calculated surface energy, followed by (220) and (200) . For CaS and SrS the order was reversed. This differs from the results of the present study (and from experimental studies referenced in Yoshiyama et al. 1988), where the lowest energy sphalerite surface is found to be $\{110\}$. However, the calculations of Yoshiyama et al. (1988) did not account for the electrostatic effects that cause the $\{111\}$ surfaces to be dipolar. With the dipole removed, the surface is no longer fully occupied as shown in Figure 3, and hence the number of dangling bonds in their analysis is incorrect. By cancelling the dipole, the number of dangling bonds for all $\{111\}$ surfaces becomes the same and rather than one or three dangling bonds per atom we have

TABLE 3. Defect configurations and formation energies, at the surface (E_s) and in the bulk (E_b) of sphalerite

Surface	Defects	E_b (eV)	E_s (eV)	E_{sg} (eV)	E_{react} (eV)	E_{eff} (Jm ⁻²)
Zn rich surfaces						
(110)	Zn _i + 2e'	16.47	15.27	-1.20	13.25	5.14
(001) S	V _s + 2e'	48.76	47.91	-0.85	8.35	4.58
(111) Zn	Zn _i + 2e'	16.47	14.74	-1.73	12.72	4.03
(110)	V _s + 2e'	48.76	46.87	-1.89	7.31	2.84
(111) S	V _s + 2e'	48.76	46.08	-0.68	8.52	2.69
(111) S	V _s + 2e'	48.76	47.29	-1.47	7.73	2.45
Zn poor surfaces						
(110)	S _i + 2h°	16.19	13.89	-2.30	9.60	3.76
(111) S	S _i + 2h°	16.19	14.81	-1.38	10.52	3.33
(001) Zn	V _{zn} + 2h°	48.75	48.06	-0.69	7.35	4.03
(110)	V _{zn} + 2h°	48.75	47.21	-1.54	6.5	2.52
(111) Zn	V _{zn} + 2h°	48.75	48.34	-0.41	7.63	2.42

Notes: E_{sg} is the segregation energy and E_{react} is the total reaction energy required to make the defective surface. The effective surface energy (E_{eff}) is the energy of the defective surface plus E_{react} .

six per four atoms. Using the treatment of Yoshiyama et al. with six dangling bonds per four surface atoms (more strictly surface sites) the energies for the {111} surfaces are calculated to be higher than those for the {220} but lower than the {200}. This result agrees with our calculations for pure surfaces and also with the experimental data quoted by Yoshiyama et al. (1988).

There is evidence that in both thin film (see Yoshiyama et al. 1988) and single-crystal growth experiments (Matsumoto and Shimaoka 1986) on sphalerite that the {111} type surfaces are most commonly observed. Therefore some mechanism must operate that is able to lower the energy of {111} with respect to {110}. Our calculations show that variations in the stoichiometry in the surface can have a pronounced effect on surface energies. When the surface is S rich (i.e., Zn vacancies) then stability of the (111) plane is favored over (110) although the energies of both are now much closer than in the perfect case. For Zn-rich surfaces (S vacancies), (111) has by far the lowest energy.

In a similar study of NiO, Oliver et al. (1995) found that the type III {111} faces could be stabilized by a change in the valence states of the surface species to produce fully occupied surface layers. We have shown here that a similar mechanism operates for ZnS. However the change in valence states of S and Zn associated with surface non-stoichiometry could equally well be achieved by the addition of impurities such as Cl⁻, Ni³⁺, and Cd³⁺. Indeed, we believe that the presence of any aliovalent impurities such as those introduced when growing crystals in a flux will have the effect of stabilizing the (111) and (111) surfaces causing them to be expressed in the morphology.

ACKNOWLEDGMENTS

K. Wright thanks NERC for financial support and the provision of computer time on Fellowship GT/94/GS.

REFERENCES CITED

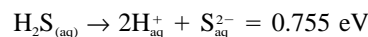
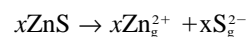
- Colbourne, E.A. (1992) Computer simulation of defects and reactions at oxide surfaces. *Surface Science Reports*, 15, 281–319.
- Davies, M.J., Parker, S.C., and Watson, G.W. (1994) Atomistic simulation of the surface structure of spinel. *Journal of Materials Chemistry*, 4, 813–816.
- Dick, B.G. and Overhauser, A.W. (1958) Theory of the dielectric constants of alkali halide crystals. *Physical Review*, 112, 90–113.
- Duke, C.B. (1988) Atomic and electronic-structure of tetrahedrally coordinated compound semiconductor interfaces. *Journal of Vacuum Science and Technology—Vacuum Surfaces and Films*, 6, 1957–1962.
- Duke, C.B. and Wang, Y.R. (1988) Surface structure and bonding of the cleavage faces of tetrahedrally coordinated II-IV compounds. *Journal of Vacuum Science Technology*, B, 6, 1440–1443.
- Duke, C.B., Paton, A., and Kahn, A. (1984) The atomic geometries of GaP (110) and ZnS (110) revisited: A structural ambiguity and its resolution. *Journal of Vacuum Science Technology*, A, 2, 515–518.
- Garcia, A. and Northrup, J.E. (1994) First-principals study of Zn and Se-stabilized ZnSe (100) surface reconstructions. *Journal of Vacuum Science Technology*, B, 12, 2678–2683.
- Kroger, F.A. (1974) The chemistry of imperfect crystals. Volume 2: Imperfection chemistry of crystalline solids. North-Holland, Amsterdam.
- Matsumoto, K. and Shimaoka, G. (1986) Crystal growth of ZnS and ZnSe by chemical transport using NH₄Cl as a transport agent. *Journal of Crystal Growth*, 79, 723–728.
- Nickel, E.H. (1965) Department of Mines and Technical Surveys, Ottawa. Information circular IC170.
- Oliver, P.M., Watson, G.W., and Parker, S.C. (1995) Molecular-dynamics simulations of nickel oxide surfaces. *Physical Review*, B52, 5323–5329.
- Parker, S.C., Titiloye, J., and Watson, G.W. (1993) Molecular modelling of carbonate minerals: studies of growth and morphology. *Philosophical Transactions of the Royal Society London*, A, 344, 37–48.
- Parry, D.E. (1975) The electrostatic potential in the surface region of an ionic crystal. *Surface Science*, 49, 433–440.
- Parry, D.E. (1976) Errata. *Surface Science*, 54, 195.
- Scott, S.D. and Barnes, H.L. (1972) Sphalerite-wurtzite equilibria and stoichiometry. *Geochimica et Cosmochimica Acta*, 36, 1275–1295.
- Tasker, P.W. (1979) The stability of ionic crystals. *Journal of Physics C: Solid State Physics*, 12, 4977–4984.
- Watson, G.W., Kelsey, E.T., de Leeuw, N.H., Harris, D.J., and Parker, S.C. (1996) Atomistic simulation of dislocations, surfaces and interfaces in MgO. *Journal of the Chemical Society, Faraday Transactions*, 92, 433–438.
- Wright, K. and Jackson, R.A. (1995) Computer simulation of the structure and defect properties of zinc sulphide. *Journal of Materials Chemistry*, 5, 2037–2040.
- Wulff, G. (1901) Zur frage de geschwindigkeit des wachstums und der auflösung der krystallflächen. *Zeitschrift für Kristallographie*, 34, 499–530.
- Yoshiyama, H., Tanaka, S., Mikami, I., Oshio, S., Nishiura, J., Kawakami, H., and Kobayashi, H. (1988) Role of surface energy in the thin-film growth of electroluminescent ZnS, CaS, and SrS. *Journal of Crystal Growth*, 86, 56–60.

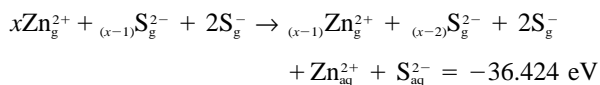
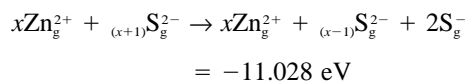
MANUSCRIPT RECEIVED JANUARY 27, 1997

MANUSCRIPT ACCEPTED SEPTEMBER 6, 1997

APPENDIX 1. DERIVATION OF REACTION ENERGIES.

ER1 and ER2



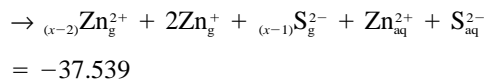
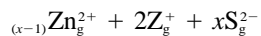
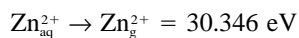
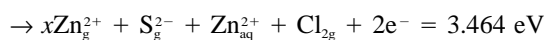
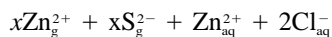
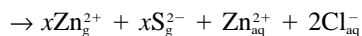
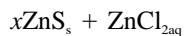


$$\text{ER1} = 0.755 + 5.988 - 11.028 - 36.424$$

$$= -40.709 \text{ eV}$$

$$\text{ER2} = 0.755 + 5.988 - 11.028 = -4.285 \text{ eV.}$$

ER3 and ER4



$$\text{ER3} = 3.464 + 30.436 - 35.92 - 37.539$$

$$= -39.559 \text{ eV}$$

$$\text{ER4} = 3.464 + 30.436 - 35.92 = -2.02 \text{ eV}$$

REFERENCE CITED

CRC Handbook of Chemistry and Physics 75th Edition (1995). D.R. Lide (Ed.)